Development of Single-Phase Shunt Active Power Filter for Reduction of Current Harmonics in Data Center Power System

Marinko Miletić
University of Zagreb, Faculty of Electrical Engineering and Computing
Zagreb, Croatia
marinko.miletic@fer.hr

Katica Raič Raguž
University of Zagreb, Faculty of Electrical Engineering and Computing
Zagreb, Croatia
katica.raic-raguz@fer.hr

Vinko Zeleničić
University of Zagreb, Faculty of Electrical Engineering and Computing
Zagreb, Croatia
vinko.zelenicic@fer.hr

Igor Erceg
University of Zagreb, Faculty of Electrical Engineering and Computing)
Zagreb, Croatia
igor.erceg@fer.hr

Damir Sumina
University of Zagreb, Faculty of Electrical Engineering and Computing
Zagreb, Croatia
damir.sumina@fer.hr

***Abstract*— In modern power systems, the integration of renewable energy sources and the increasing use of power electronic devices can lead to harmonic distortions, imbalances and other power quality issues. These issues can lead to equipment failures, overheating and increased energy losses. Active filters can mitigate these issues by injecting a compensating current into the power system to compensate for harmonics and improve the power factor. Shunt Active Power Filters (SAPF) play an important role in the smart grid by helping to improve power quality. The aim of this paper is to present a simple model of a SAPF that has one current control loop with an LCL filter output current as a feedback signal and a PI controller. The development of the prototype model and its design with all the necessary parameters to build a simulation model are presented in detail. The simulation model is also verified experimentally and a comparison between the simulation and experimental results is presented.**

Keywords—harmonic distortion, shunt active power filter, smart grid, power quality, LCL filter.

I. INTRODUCTION

Current harmonics are an increasing problem in systems with many nonlinear loads. Shunt Active Power Filters (SAPF) effectively solve the problem of current harmonic [1]. In SAPF, L and LCL filters are used at the output to filter the pulsating voltage and reduce the switching harmonics. Compared to the classical L filter, the LCL is preferred because of its more remarkable ability to attenuate high-frequency harmonics, as the capacitor behaves like a short circuit at high frequencies. However, using an LCL filter can cause the system to be unstable, so specific methods are needed to stabilize the control system. There are two methods, passive and active damping. Passive damping is achieved by adding a damping resistor in series with the capacitor. The method is very simple and reliable [2], but results in additional resistive losses and degrades the ability to damp harmonics. With active damping, the apparent resistance R is simulated by returning the variables as damping terms. Active damping is widely used because of its flexibility and efficiency, but additional sensors are needed, increasing the implementation complexity [3]. In this paper, passive damping is considered. It is necessary to pay special attention to component selection because if the system inductance is too large, the LCL interface filter can effectively suppress the high-frequency ripple of the converter output current. Still, the system inertia will be more significant, and the dynamic response speed of the system will be slower. If the value of the system inductance is small, suppressing output current high-frequency harmonics will be worse [4].

An example of an LCL filter with passive damping can be found in [5]. The load is represented as an active DC-traction power plant with an uncontrolled 12-pulse rectifier. The positive effect of the damping resistor is mainly to reduce the gain around the resonant frequency and to improve stability by eliminating the oscillations. The simulation model of the system was created using the Matlab/Simulink software package. Before compensation, the line current in the secondary circuit is almost rectangular, with a total harmonic distortion (THD) of 28.36%. When used in an active substation DC, the LCL filter designed according to the proposed algorithm reduced switching harmonics by about 71%.

The design procedure of the LCL filter for Active Power Filter (APF) is presented in [6]. An active damping control strategy was used to suppress resonance that utilizes the filter capacitor's current feedback. A smaller total inductance was used to achieve the required damping. To simplify the controller, automatic pole-zero suppression was uncovered, and the pole-zero mapping method was used for controller tuning. The results confirmed the simplicity of implementation and good control performance.

SAPF system connected to the PCC via an LCL filter in a three-phase system is presented in [7]. The LCL filter model has taken the phase lag into account. The modulation index of the SAPF converter has been set to a high value (greater than 0.9). The reactive current setpoint was set to zero, and the grid currents' fundamental components were controlled with a proportional-integral controller in the synchronous *dq* frame. The prototype SAPF system has been built to test it in practice. The experimental results showed that the grid current THD after compensation was 3.49%, while the THD of the nonlinear load current could be as high as 40.37%.

Active power filters contain two cascaded control loops. The inner current loop is responsible for tracking a reference current, and the outer loop controls the DC bus voltage. DC bus voltage control method based on a Second-Order Generalised Integrator (SOGI), is presented in [8]. The SOGI

This work has been fully supported by the European Regional Development Fund under the project "Development of a system for optimizing power consumption in data centers" (KK.01.2.1.02.0082).

acts as a band-stop filter, and the current controller has evolved from the proportional resonance controller (PR). A simulation study was carried out using PLECS software to validate the proposed method. The results show that the proposed method is superior to the conventional method in harmonic suppression. It was shown that the transient response of the system was not affected.

The simple structure of the control system and the control with inverter current as current feedback signal are shown in [9]. The control system consists of a control loop with a controller of the PI type and another control loop with virtual damping (resistor). The responses are given for grid and inverter currents as feedback signals. With the inverter current as current feedback signal, the SAPF becomes sensitive to external influences.

A SAPF with passive damping and an electrical and block diagrams, practically identical to that presented in this paper, is presented in [10]. The current control system has an internal loop with a PI controller and an external loop with a repetitive controller. The THD of the load current is 38% and with the applied control, the grid current THD is 1.6%.

An example of current control with inverter current as current feedback signal can be found in [11]. With this current, active damping was carried out. SAPF with passive damping and two current control loops is presented in [12]. The inner control loop consists of a PI controller and the outer one of a repetitive controller. The responses and the THD value for the inner control loop are given. The grid current THD is 14%.

This paper presents the SAPF prototype with an LCL filter for reducing current harmonics in data centers. The advantages of this SAPF are the simplicity of the circuit design and the simplicity of the control loop. The active filter has only one feedback loop and a classic PI controller. The entire control system is implemented in analogue technology. The paper is divided into five sections. The first section contains an introduction and related work. The second section presents the system analysis using transfer functions. The SAPF design with detailed parameters for each component is presented in the third section and the experimental verification is in the fourth section. The conclusion follows in the fifth section.

II. SYSTEM ANALYSIS

The SAPF circuit diagram is shown in Fig. 1. SAPF comprises a two-level Voltage Source Inverter (VSI) with DC capacitors and an LCL-type output filter. L_1 is the inverter-side filter inductor, L_2 is the grid-side filter inductor, and C is the filter capacitor. The LCL filter output current (i_2) or the VSI current (i_1) can be used as the current feedback signal. This paper uses the LCL filter output current as the feedback signal.

A SAPF control diagram for filtering higher current harmonics is shown in Fig. 2.**Hata! Başvuru kaynağı bulunamadı.** The current command is composed of the harmonic component i_h and active current i_{2dc} required to keep the DC side capacitor voltage u_{dc} constant. The current i_2 is a sinusoidal current in phase with the voltage u_s. The voltage controller determines the i_2 amplitude to compensate for the power loss of the SAPF. A detailed current control loop is shown in Fig. 3.

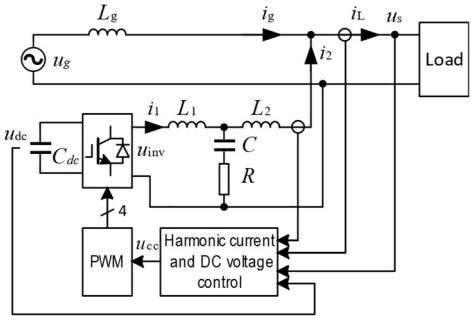

Fig. 1. Circuit diagram of SAPF with LCL output filter

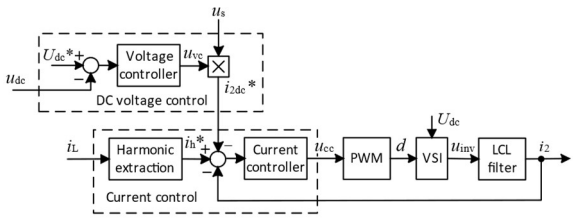

Fig. 2. Shunt Active Power Filter control diagram

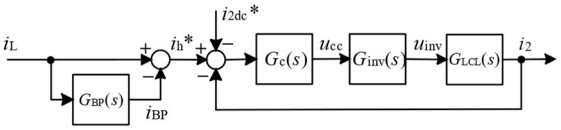

Fig. 3. Current control loop diagram

The system has two loops: one dc-bus voltage outer loop and one current inner loop. As the outer loop has little influence on the system stability, it can be excluded from the system stability analysis, and only the current control is considered.

The load current is represented as the sum of the fundamental and the higher harmonics:

$$i_L(t) = I_{L1}\sin(\omega_g t + \varphi_1) + \sum_{h=2}^{\infty} I_{Lh}\sin(h\omega_g t + \varphi_h) = i_{L1}(t) + i_h(t) \quad (1)$$

If $i_2 = i_h$ applies to the SAPF current, then the grid current is (Fig. 1):

$$i_g = i_L - i_2 = (i_{L1} + i_h) - i_h = i_{L1} \quad (2)$$

The fundamental current harmonic signal i_{L1} is separated from current signal i_L using a bandpass filter. Bandpass filter output signal is i_{BP}. By subtracting the i_{BP} signal from the i_L signal, one obtains the current harmonic demand signal i_h^*.

The bandpass filter transfer function is given in Eq (3). The filer resonant (center) frequency is equal to the grid frequency ω_g, and the slope of the frequency response in its vicinity and the bandwidth ω_{BW} are determined by the quality factor Q. The coefficient k is set to the value $k = 1/Q$ so that the gain of the filter at the resonance frequency ω_g is equal to one. The bandwidth is given by Eq. (4).

$$G_{BP}(s) = \frac{i_{BP}(s)}{i_L(s)} = \frac{k\frac{s}{\omega_g}}{\frac{s^2}{\omega_g^2} + \frac{1}{Q}\frac{s}{\omega_g} + 1} \quad (3)$$

$$\omega_{BW} = \omega_g / Q \quad (4)$$

The transfer function of the LCL filter, where $L = L_1 \parallel L_2$, is given:

$$G_{LCL}(s) = \frac{i_2(s)}{u_{inv}(s)} = \frac{1}{(L_1 + L_2)s} \cdot \frac{RCs + 1}{LCs^2 + RCs + 1} \quad (5)$$

Using the general form of the second-order polynomial, using the natural frequency ω_n and the relative damping factor ζ, the following transfer function is obtained:

$$G_{LCL}(s) = \frac{1}{(L_1 + L_2)s} \cdot \frac{2\zeta\frac{s}{\omega_n} + 1}{\frac{s^2}{\omega_n^2} + 2\zeta\frac{s}{\omega_n} + 1} \quad (6)$$

$$\omega_n = \frac{1}{\sqrt{LC}} \quad (7)$$

$$\zeta = \frac{R}{2}\sqrt{\frac{C}{L}} \quad (8)$$

With $\zeta > 1$, the second-order polynomial in the denominator of Eq. (6) has two real roots:

$$G_{LCL}(s) = \frac{1}{(L_1 + L_2)s} \cdot \frac{RCs + 1}{\left(\frac{s}{\omega_1} + 1\right)\left(\frac{s}{\omega_2} + 1\right)} \quad (9)$$

$$\omega_1 = \omega_n\left(\zeta - \sqrt{\zeta^2 - 1}\right) \quad (10)$$

$$\omega_2 = \omega_n\left(\zeta + \sqrt{\zeta^2 - 1}\right) \quad (11)$$

$$\omega_1\omega_2 = \omega_n^2 \quad (12)$$

$$\omega_3 = \frac{1}{2\zeta}\omega_n \quad (13)$$

where ω_1 and ω_2 are determined by Eq. (10) and Eq. (11). The frequencies ω_1 and ω_2 are symmetrical about ω_n (on a logarithmic scale) and their product is given by Eq. (12). Frequency ω_3 is given by Eq. (13).

If $\zeta^2 \gg 1$, then according to Eq. (11) $\omega_2 \approx 2\zeta\omega_n$. It follows from Eq. (12) $\omega_1 \approx (1/2\zeta)\omega_n = \omega_3$. In this case, the transfer function $G_{LCL}(s)$ is simplified:

$$G_{LCL}(s) \approx \frac{1}{(L_1 + L_2)s} \cdot \frac{1}{\frac{s}{\omega_2} + 1} \quad (14)$$

and contains only one cut-off frequency, ω_2.

The PWM circuit controls the operation of the transistor switches in VSI and determines the output voltage u_{inv}. The circuit can be modelled as a transfer function using a proportional term with a dead time or as a first-order equivalent system. The latter has been used:

$$G_{inv}(s) = \frac{u_{inv}(s)}{u_{cc}(s)} = \frac{k_{inv}}{T_{inv,ekv}s + 1} \quad (15)$$

The time constant $T_{inv,ekv}$ is the equivalent value resulting from the method of generating the output voltage u_{inv}, while the gain $k_{inv} = U_{dc}/U_m$, where U_{dc} stands for the DC supply voltage and U_m for the triangular carrier signal peak value in the PWM.

The transfer function $G_P(s)$, from the current controller output u_{cc} to the SAPF output current i_2, is given by:

$$G_P(s) = \frac{i_2}{u_{cc}} = G_{inv}(s)G_{LCL}(s) = \frac{k_{inv}}{T_{inv,ekv}s + 1}G_{LCL}(s) \quad (16)$$

$$G_P(s) \approx \frac{k_{inv}}{(L_1 + L_2)s} \cdot \frac{1}{\frac{s}{\omega_2} + 1} \quad (17)$$

If the breaking frequency $1/T_{inv,ekv}$ is far away from the frequency range of interest, the time constant $T_{inv,ekv}$ can be neglected, and $G_P(s) \approx k_{inv}G_{LCL}(s)$ can be used. Further simplification of the transfer function $G_{LCL}(s)$, according to Eq. (14), leads to Eq. (17).

III. SAPF DESIGN

Taking into account the real needs of a data center, the requirements for the design of a single-phase active filter for a voltage of 230V, 50Hz and a current of 4A were defined.

A. LCL filter

In accordance with the requirements, the parameters of the LCL filter were determined (Table 1).

B. Harmonic extraction

Bandpass filter Q value is set to 20. At the frequency of the third harmonic, the gain is $|G_{BP}| = 0{,}0187 = -34{,}5\ dB$, which means that the current signal i_{BP} contains also a small part of the third harmonic. This also applies to all other higher harmonics. The proportion of harmonics is inversely proportional to the order of the harmonics h. Therefore, the current signal $i_h^* = i_L - i_{BP}$ does not contain the exact amplitude value of each harmonic amplitude but a slightly smaller value. For $h = 3$, the amplitude ratio is 0.98. With increasing h, the ratio rises toward 1. From a technical point of view, these differences are insignificant.

The frequency response for the bandpass and the entire *Harmonic extraction* block are shown in Fig. 4. The blue waveform represents the frequency response of the bandpass filter (i_{BP}/i_L), and the red waveform represents the frequency response of the extraction block (i_h^*/i_L).

C. PWM and VSI

The frequency of the triangular carrier signal is $f_{sw} = 30\ kHz$, and the amplitude $U_m = 9{,}5\ V$. The DC supply voltage is $U_{dc} = 400\ V$; so $k_{inv} = U_{dc}/U_m = 42$. The time constant $T_{inv,ekv}$ can be ignored.

D. Current controller

The controller $G_c(s)$ should be such that the following is fulfilled (for the open loop $G_o(s) = G_c(s) \cdot G_p(s)$):

- the phase margin is greater than 30°,
- the unity-gain crossover frequency f_c is less than $0.25 \cdot f_{sw}$
- the gain at frequency f_{sw} is less than -14dB, and
- the unity-gain crossover frequency f_c is on the part of the characteristic with a slope of -20dB/dec.

The specified requirements are already achieved with the P controller, $G_c(s) = k_p$. The addition of an integral part increases the gain in the frequency range in which the harmonics are located, which has a favorable effect on the accuracy. Therefore, the controller of type PI is chosen (Eq. (18)) with parameters $k_p = 0.23$ and $T_i = 0.23\,ms$ ms is used.

$$G_c(s) = k_p \cdot \frac{1 + sT_i}{sT_i} \tag{18}$$

The cut-off frequency of the controller is $\omega_{PI} = 4.44 \cdot 10^3\ rad/s$, i.e., $f_{PI} = 700\ Hz$.

E. Simulation results

This subsection shows the responses of current harmonic filtering in a circuit according to (Fig. 1.). Simulation model was created in the PLECS software package and accurately represents the operation of PWM and VSI. The power grid is represented as a voltage source in series with the grid impedance. The grid parameters are $U_g = 230\ V_{rms}$, $f_g = 50\ Hz$ and $L_g = 1.4\ mH$.

The nonlinear load is a diode rectifier with RL load on the DC side. The current waveform on the diode rectifier AC side is rich in harmonics and is therefore suitable for SAPF experimental verification. Such a load is commonly used to obtain current harmonics in experimental verification. The values for the resistance and inductance are 100 Ω and 400 mH respectively.

Table 1. LCL parameters

Parameter	*Value / Unit*
L_1	2 mH
L_2	0,5 mH
C	8 µF
R	20 Ω
$L=L_1 \| L_2$	0,4 mH
ω_n	$17{,}68x10^3$ rad/s
f_n	2,81 kHz
ζ	1,414
ω_1	$7{,}32x10^3$ rad/s
ω_2	$42{,}7x10^3$ rad/s
ω_3	$6{,}25x10^3$ rad/s
f_1	1,17 kHz
f_2	6,8 kHz
f_3	0,995 kHz

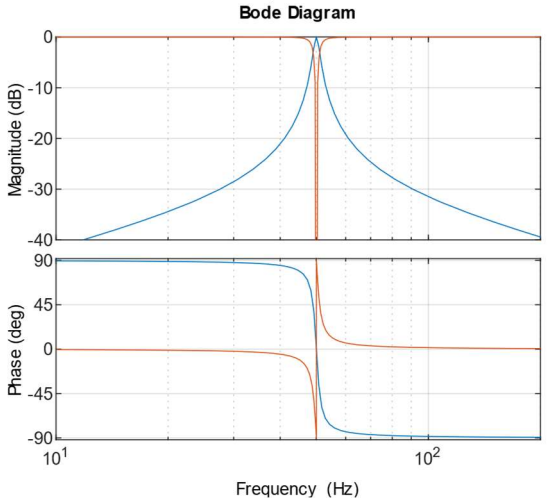

Fig. 4. Bandpass filter frequency response

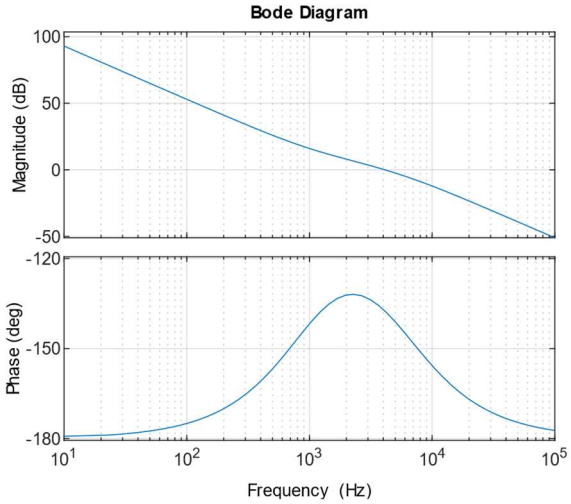

Fig. 5. Open loop frequency response

The load current i_L (blue) and APF current i_2 (red) waveforms are shown in Fig. 6., while Fig. 7. shows the grid current i_g waveform. The load current RMS value is 2.09 A and the grid current RMS value is 1.98 A. The load current THD is 38.9% and the grid current THD after filtering is 1.8% (**Hata! Başvuru kaynağı bulunamadı.**.). The simulation results show that the grid current THD in the system with the SAPF is reduced by 27dB compared to the system without SAPF.

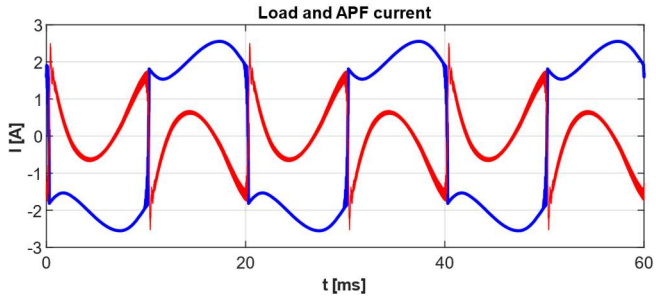

Fig. 6. Load (blue) and APF (red) current waveforms

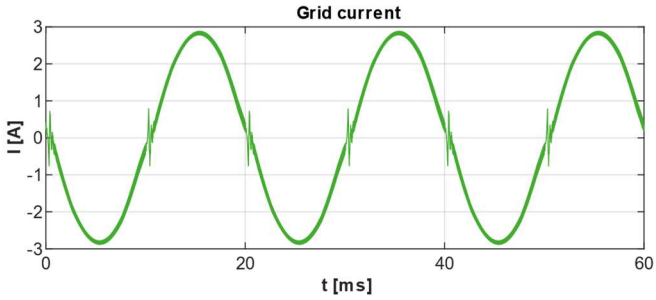

Fig. 7. Grid current waveform

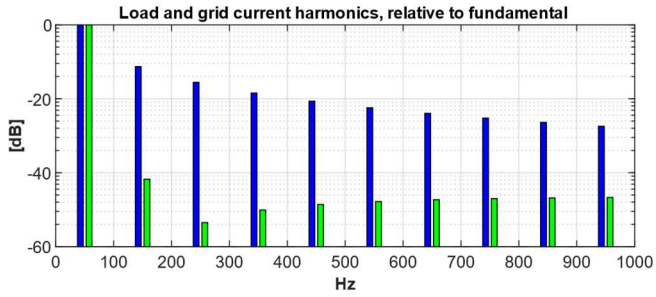

Fig. 8. Load and grid current harmonics

IV. Experimental verification

The grid for the experimental verification is realized using a regulating transformer (replaced in the simulation by a voltage source and a reactance). The load was realized in the way described in the chapter "Simulation results". The SAPF prototype consists of a control circuit, a power circuit, and an output filter (**Hata! Başvuru kaynağı bulunamadı.**.). The entire control system is implemented in analogue technology with the parameters described in the chapter "SAPF design". The measurements were carried out with a *Dewesoft data acquisition system (SIRIUS XHS). Dewesoft DS-CLAMP 500 DC* current sensors with a sampling frequency of 100kHz were used to measure the current.

Fig. *1***Hata! Başvuru kaynağı bulunamadı.**. shows the load current (blue) and APF current (red) waveforms, while **Hata! Başvuru kaynağı bulunamadı.**. shows the grid current waveform. The load current RMS value is 1.917 A and the grid current RMS value is 1.815 A. The load current THD is 38.4% and the grid current THD after filtering is 2.4% (**Hata! Başvuru kaynağı bulunamadı.**).

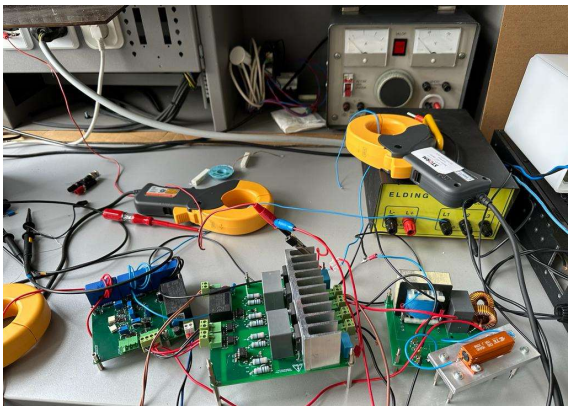

Fig. 9. Experimental setup

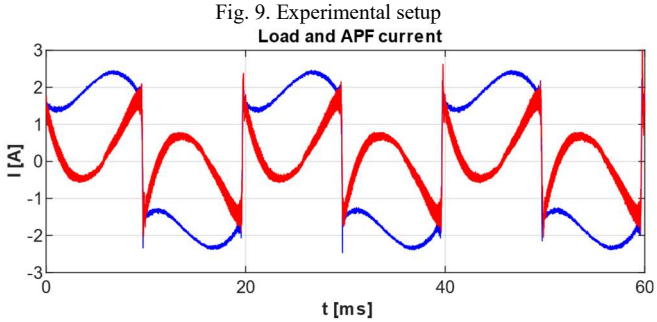

Fig. 10. Load (blue) and APF (red) current waveforms

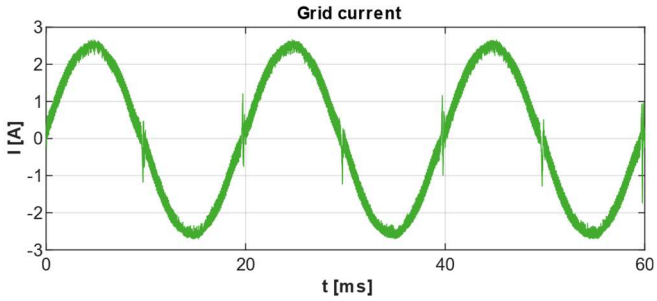

Fig. 11. Grid current waveform

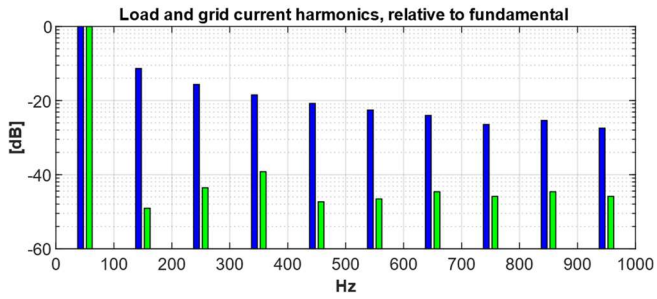

Fig. 12. Load and grid current harmonics

The measured load current THD on the SAPF prototype has a value of 38%, as in the simulation, and the measured grid current THD is 2.4%, while the grid current THD determined by the simulation is 1.8%. The experimental results show that the grid current THD in the system with the SAPF is reduced by 24dB compared to the system without SAPF.

V. Conclusion

The paper presents the design of a Shunt Active Power Filter prototype for reducing current harmonics in data centers. The active filter has one current control loop with an LCL filter output current as a feedback signal, and a PI controller. A simulation model was created with the PLECS software package and then verified experimentally. The entire control system is implemented in analogue technology. A comparison was made between simulation and experimental results. The results show an attenuation of at least 20 dB for each harmonic up to the 25th harmonic. For a load with a current THD of 38%, the active filter reduces the THD of the grid current to below 2.5%.

REFERENCES

[1] K. R. Raguž, M. Miletić, V. Zeleničić, D. Sumina, I. Erceg and Ž. Nastasić, "Analysis of current harmonics in data center power system," 2022 45th Jubilee International Convention on Information, Communication and Electronic Technology (MIPRO), Opatija, Croatia, (2022), pp. 153-157

[2] M. Büyük, A. Tan, K. Ç. Bayindir, and M. Tümay, "Analysis and comparison of passive damping methods for shunt active power filter with output lcl filter," in 2015 Intl Aegean Conference on Electrical Machines & Power Electronics (ACEMP), 2015 Intl Conference on Optimization of Electrical & Electronic Equipment (OPTIM) & 2015 Intl Symposium on Advanced Electromechanical Motion Systems (ELECTROMOTION). IEEE, 2015, pp. 434–440.

[3] L. Yang and J. Yang, "A Robust Dual-Loop Current Control Method With a Delay-Compensation Control Link for LCL-Type Shunt Active Power Filters," in IEEE Transactions on Power Electronics, vol. 34, no. 7, pp. 6183-6199, (2019)

[4] L. Zhou, Z. Liu, Y. Ji, D. Ma, J. Wang and L. Li, "A Improved Parameter Design Method of LCL APF Interface Filter," 2020 IEEE International Conference on Artificial Intelligence and Computer Applications (ICAICA), Dalian, China, (2020), pp. 948-952

[5] M. Popescu, A. Bitoleanu and V. Suru, "On the design of LCL filter with passive damping in three-phase shunt active power filters," 2016 International Symposium on Power Electronics, Electrical Drives, Automation and Motion (SPEEDAM), Capri, Italy, (2016), pp. 825-830

[6] Guohong Zeng, T. W. Rasmussen, Lin Ma and R. Teodorescu, "Design and control of LCL-filter with active damping for Active Power Filter," 2010 IEEE International Symposium on Industrial Electronics, Bari, Italy, (2010), pp. 2557-2562

[7] Y. Tang, P. C. Loh, P. Wang, F. H. Choo, F. Gao and F. Blaabjerg, "Design, control, and implementation of LCL-filter-based shunt active power filters," 2011 Twenty-Sixth Annual IEEE Applied Power Electronics Conference and Exposition (APEC), Fort Worth, TX, USA, (2011), pp. 98-105

[8] M. Kale, F. Akar and M. Karabacak, "A SOGI Based Band Stop Filter Approach for a Single-Phase Shunt Active Power Filter," 2018 2nd International Symposium on Multidisciplinary Studies and Innovative Technologies (ISMSIT), Ankara, Turkey, (2018), pp. 1-4

[9] W. Zhao, Y. Li, and G. Chen, "A double-loop current control strategy for shunt active power filter with lcl filter," in 2009 IEEE International Symposium on Industrial Electronics, 2009, pp. 1841– a1845.

[10] Y. Zhang, Z. Dai and Y. Fang, "Voltage Feed Forward Shunt Active Power Filter Based On Double Loop Control," 2021 International Conference on Power System Technology (POWERCON), Haikou, China, 2021, pp. 1251-1256

[11] H. Yuan and X. Jiang, "A simple active damping method for Active Power Filters," 2016 IEEE Applied Power Electronics Conference and Exposition (APEC), Long Beach, CA, USA, 2016, pp. 907-912

[12] C. Xie, Z. Wang and G. Chen, "A simple method of realization of low power loss and high compensation-precision active power filter," 2009 International Conference on Sustainable Power Generation and Supply, Nanjing, China, 2009, pp. 1-5